

NRC Publications Archive Archives des publications du CNRC

Roll reduction control system characteristics of a vessel equipped with z-drives

Millan, J.; Thistle, S.; Thornhill, E.; Stredulinsky, D.

This publication could be one of several versions: author's original, accepted manuscript or the publisher's version. / La version de cette publication peut être l'une des suivantes : la version prépublication de l'auteur, la version acceptée du manuscrit ou la version de l'éditeur.

Publisher's version / Version de l'éditeur:

8th Canadian Marine Hydromechanics and Structures Conference [Proceedings], 2007

NRC Publications Archive Record / Notice des Archives des publications du CNRC :

<https://nrc-publications.canada.ca/eng/view/object/?id=907e5c40-ddd9-4ac0-8c32-5891b15eb419>

<https://publications-cnrc.canada.ca/fra/voir/objet/?id=907e5c40-ddd9-4ac0-8c32-5891b15eb419>

Access and use of this website and the material on it are subject to the Terms and Conditions set forth at

<https://nrc-publications.canada.ca/eng/copyright>

READ THESE TERMS AND CONDITIONS CAREFULLY BEFORE USING THIS WEBSITE.

L'accès à ce site Web et l'utilisation de son contenu sont assujettis aux conditions présentées dans le site

<https://publications-cnrc.canada.ca/fra/droits>

LISEZ CES CONDITIONS ATTENTIVEMENT AVANT D'UTILISER CE SITE WEB.

Questions? Contact the NRC Publications Archive team at

PublicationsArchive-ArchivesPublications@nrc-cnrc.gc.ca. If you wish to email the authors directly, please see the first page of the publication for their contact information.

Vous avez des questions? Nous pouvons vous aider. Pour communiquer directement avec un auteur, consultez la première page de la revue dans laquelle son article a été publié afin de trouver ses coordonnées. Si vous n'arrivez pas à les repérer, communiquez avec nous à PublicationsArchive-ArchivesPublications@nrc-cnrc.gc.ca.

Roll Reduction Control System Characteristics of a Vessel Equipped With Z-Drives

J. Millan^{1*}, S. Thistle², E. Thornhill³ and D. Stredulinsky³

¹ *Institute for Ocean Technology, National Research Council Canada, St. John's, NL, A1B 3T5, Canada*

² *Memorial University of Newfoundland, St. John's, NL, A1B 3T5, Canada*

³ *Defense Research and Development Canada Atlantic, Dartmouth, NS, B2Y 3Z7, Canada*

Email: jim.millan@nrc-cnrc.gc.ca

ABSTRACT

This paper examines the control system characteristics of a vessel that uses Z-drives to actively reduce roll motion. Active roll control systems that use rudders and fins have been in existence for many years and the capabilities of such systems have been studied extensively. As an actuator, the Z-drive suffers from many of the same limitations as rudders; for example, the vessel's steering is also closely linked to the rudder motion. The Z-drive has an advantage over rudders and many fin-based systems in that it has the potential to be an effective actuator for roll motion reduction at low and even zero forward speeds: conditions in which a rudder is completely ineffective. Full-scale trial data is used to establish some design principles for a roll reduction system based on Z-drive operation.

1 INTRODUCTION

Before considering the effectiveness of a Z-Drive as a roll reduction system, it is useful to look at the closely related area of rudder-actuated roll reduction systems. Extensive research has been conducted in the area of rudder roll stabilizing (RRS) systems, and the associated control theory, beginning in the 1970's [3]. Interestingly, the early work was inspired by the observation that a poorly tuned autopilot actually induced anomalous roll motions [8]. Although some initial results were successful [4], it became clear early on that roll reduction was not universally effective, being strongly influenced by limitations of the steering gear and the relatively large roll inertia of some vessels. A serious limitation to RRS is the fact that the dynamics of the rudder-to-roll response are non-minimum phase (NMP) [7], which results in a tradeoff between reduc-

ing roll at some frequencies, while amplifying it at others.

In a RRS system, the control system manipulates only one system input, the rudder angle, in order to control both the yaw and the roll: thus the system is under-actuated. With a Z-drive vessel, an additional degree of freedom is available for control: the propeller shaft speed. This is an important distinction in two ways: the additional degree of control can be used at forward speeds to improve the actuation, and it permits roll to be controlled even at low to zero forward speed, when rudders are useless in this capacity. This idea was investigated in an earlier paper [9], in which a roll stabilization control system was tested on a simulated vessel. The results indicated (as one might expect) that Z-drives had some potential for roll reduction at forward speeds. In that study, the zero-speed characteristics were not studied, and no particular emphasis was placed on the control system design aspects. This paper will focus on the modeling of a Z-drive vessel for the purpose of developing Z-drive roll stabilization (ZRS) and yaw control system.

This paper is organized as follows: Section 2 gives an overview of the control system models that are used for control system design. Section 3 describes the techniques used to identify the vessel model from full-scale trials data. Section 4 presents the results of the modeling and the implication for controller design. Finally, Section 5 summarizes the results and suggests directions for future work.

2 VESSEL MODELING

In order to develop a control system for a vessel, it is desirable to have a suitable linearized model of the behaviour over a range of operating conditions, thus

*Sponsoring Organization

enabling modern multivariable control system design techniques to be utilized [10]. Typically, such a model begins with a Newtonian formulation of the equations of motion, yielding a set of nonlinear relations. Such an approach requires that the hydrodynamics and hydrostatics of the vessel be known; in this paper, the vessel is examined from a control system design standpoint and the model is identified from actual sea trials data.

2.1 Sway-Yaw and Roll Model

The model of Christensen and Blanke [2] is derived by linearizing a nonlinear 3 degrees-of-freedom (DOF) manoeuvring model about the forward service speed $u = u_0$, and then rearranging it into a standard state space form:

$$\dot{\mathbf{x}} = \mathbf{A}\mathbf{x} + \mathbf{B}\delta \quad (1)$$

where the state vector is defined as $\mathbf{x} = [v, r, p, \phi, \psi]^T$ with the state variables defined respectively: sway velocity, roll rate, yaw rate, roll angle and yaw angle. Note that $\dot{\phi} = p, \dot{\psi} = r$. The elements a_{ij} and b_i of \mathbf{A} and \mathbf{B} are to be determined by experimental techniques (i.e. system identification), they will not be defined, since they will act as placeholders for the system identification. Thus Eqn. 1 is expanded as follows:

$$\begin{bmatrix} \dot{v} \\ \dot{r} \\ \dot{p} \\ \dot{\phi} \\ \dot{\psi} \end{bmatrix} = \begin{bmatrix} a_{11} & a_{12} & a_{13} & a_{14} & 0 \\ a_{21} & a_{22} & a_{23} & a_{24} & 0 \\ a_{31} & a_{32} & a_{33} & a_{34} & 0 \\ 0 & 0 & 1 & 0 & 0 \\ 0 & 1 & 0 & 0 & 0 \end{bmatrix} \begin{bmatrix} v \\ r \\ p \\ \phi \\ \psi \end{bmatrix} + \begin{bmatrix} b_1 \\ b_2 \\ b_3 \\ 0 \\ 0 \end{bmatrix} \delta$$

It is useful to decompose the roll and the sway-yaw dynamics in order to separate the effects of the rudder on each of roll and yaw. Rearranging the state variables $\mathbf{x} = [v, r, \psi, p, \phi]^T$ the system matrices rearrange as follows:

$$\mathbf{A} = \left[\begin{array}{cc|cc} a_{11} & a_{12} & 0 & a_{13} & a_{14} \\ a_{21} & a_{22} & 0 & a_{23} & a_{24} \\ 0 & 1 & 0 & 0 & 0 \\ \hline a_{31} & a_{32} & 0 & a_{33} & a_{34} \\ 0 & 0 & 0 & 1 & 0 \end{array} \right] \quad (2)$$

$$\mathbf{B} = [b_1 \quad b_2 \quad 0 \mid b_3 \quad 0]^T \quad (3)$$

In the partitioned matrix \mathbf{A} of Eqn. 2, the upper left partition represents the dynamics of the vessel steering which can be recognized as the 2nd order Nomoto model. The lower right partition models the behaviour of the vessel in roll, and the upper right and lower left partitions represent the coupling between the sway-yaw and roll subsystems. In some cases, the coupling

is neglected to simplify the model further [5]. In our case, coupling will be retained in order to improve the results of the system identification process.

2.2 Roll Mode Modeling

For purposes of system identification, the model is further augmented to separate the roll behaviour into low and high frequency components ϕ_{lf} and ϕ_{hf} . This is because the roll stabilizing controller will only operate around the high frequencies; i.e. that of the resonant pole pair represented by the underdamped harmonic oscillator. The low frequency roll behaviour can be modeled by an additional pair of overdamped poles (eigenvalues). As a result, the roll subsystem transfer function will look as follows:

$$\frac{\phi(s)}{\delta(s)} = \frac{K_{roll}(s - z_1)(s + z_2)}{\underbrace{(s - p_1)(s + p_2)}_{lfmodel} \underbrace{(s^2 + 2\zeta\omega_n s + \omega_n^2)}_{hfmodel}} \quad (4)$$

The high frequency model has been written in the form of a damped harmonic oscillator to facilitate the identification of the damping ζ and the natural frequency ω_n . The latter corresponds to the natural roll frequency ω_ϕ of the vessel, while the former is the non-dimensional damping of the complex conjugate pole pair. The complex conjugate pole locations are given in terms of the damping and natural frequency as follows:

$$p_3, p_4 = -\omega_n \zeta \pm j\omega_n \left(\sqrt{1 - \zeta^2} \right)$$

Appearing in the numerator are a pair of zeroes z_1, z_2 , where z_1 is the right-half plane zero that contributes the NMP dynamics of the system. A state-space version of the roll subsystem with state vector $\mathbf{x}_\phi = [p_{hf}, \phi_{hf}, p_{lf}, \phi_{lf}]^T$ takes the form

$$\mathbf{A}_\phi = \left[\begin{array}{cc|cc} -2\zeta\omega_n & \omega_n^2 & 0 & 0 \\ 1 & 0 & 0 & 0 \\ \hline 0 & 0 & -(p_1 + p_2) & -p_1 p_2 \\ 0 & 0 & 1 & 0 \end{array} \right] \quad (5)$$

$$\mathbf{B}_\phi = [b_{\phi 1} \quad 0 \mid b_{\phi 3} \quad 0]^T \quad (6)$$

Augmenting the state vector appropriately $\mathbf{x} = [v, r, \psi, \mathbf{x}_\phi]^T$ and inserting this new roll model into the system of Eqn. 2 and 3, the model becomes

$$\mathbf{A} = \left[\begin{array}{c|c} \mathbf{A}_{11} & \mathbf{L}_1 \\ \hline \mathbf{L}_2 & \mathbf{A}_\phi \end{array} \right] \quad (7)$$

$$\mathbf{B} = \left[\begin{array}{c} \mathbf{B}_1 \\ \hline \mathbf{B}_\phi \end{array} \right] \quad (8)$$

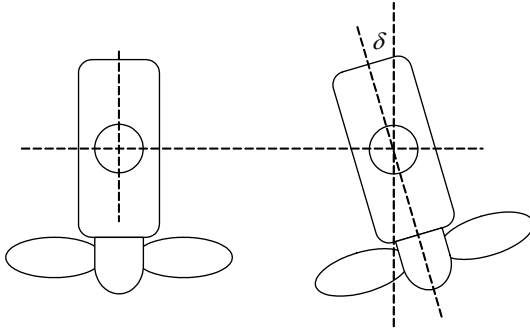


Figure 1: Independent steering mode - one Z-drive azimuth angle δ is used for steering and roll compensation

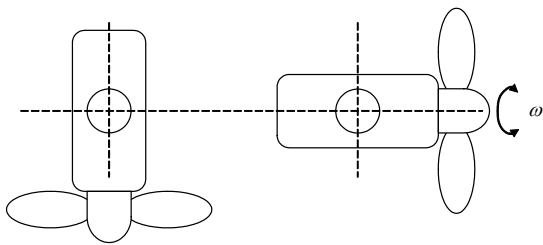


Figure 2: Side thruster mode - one Z-drive shaft speed ω_s is used for positioning and roll compensation

where \mathbf{A}_{11} is the upper partition of Eqn. 2 and \mathbf{L}_1 and \mathbf{L}_2 are cross-coupling, and are structured such that only the low frequency roll states couple to the sway-yaw states. Matrix \mathbf{B}_1 is the upper portion of Eqn. 3.

2.3 Control Actuator Modes

The target vessel is equipped with two independently controlled Z-drives. Thus, it is possible to vary both the azimuth angle δ of the drives and the shaft speed ω_s completely independently. For the purpose of this study, the drives were operated in three distinct modes: 1) *locked mode*, in which both Z-drives are used like a rudder with the same azimuth command δ , 2) *independent mode* either port or starboard drives are used as a rudder, e.g. $\delta_{port} = 0$ $\delta_{stbd} = \delta$ (see Fig. 1) and 3) *side thruster mode* one thruster is placed athwartship e.g. $\delta_{port} = 90$ degrees and the shaft speed is varied (see Fig. 2). Modes 1 and 2 are used for forward speed steering and roll reduction, while mode 3 is used for zero or very low speeds positioning and roll reduction.

In practice, it is likely that the thrusters would be operated so that the controller would be free to vary both shaft speeds and azimuths in order to optimize the con-

trol. The above operating modes were investigated as representing 2 extremes of operation; i.e cruise speeds $u > 0$ and stationkeeping to low-speed manoeuvring $u \approx 0$. For mode 3, the model used for SI purposes is

$$\dot{\mathbf{x}} = \mathbf{A}_\phi \mathbf{x} + \mathbf{B}_\phi \omega_s \quad (9)$$

where \mathbf{A}_ϕ and \mathbf{B}_ϕ are of a similar structure to that defined by Eqn. 5 and 6 respectively, with the shaft speed ω_s the input to the system.

3 SYSTEM IDENTIFICATION

System identification (SI) refers to the process of identifying the parameters of a model based on the observation of the inputs and outputs to the system [6]. In the previous section, a linear 3DOF model that is suitable for ZRS was developed.

3.1 Sea Trials

The sea trials conducted on the target vessel were designed to identify the vessel manoeuvring characteristics, with a particular emphasis placed on system identification of roll and yaw characteristics. In [1], Blanke and Knudsen outline some standard and non-standard manoeuvres aimed at ship manoeuvring model identification. They compare the suitability of a variety of these maneuvers using a sensitivity approach. The standard zig-zag manoeuvre was found to be one of the better techniques for this purpose. Thus, many of the runs during the sea trial were zig-zags conducted using steering modes 1 and 2 for three different forward speeds and a variety of rudder and heading step sizes. Additional runs were used to identify the zero-speed ship behaviour as well, using steering mode 3. These consisted essentially of a series of pseudo-random step changes in shaft speed with one of the Z-drives set athwartship.

3.2 Data Analysis

The MATLAB system identification toolbox was used to analyze the sea trial data, using the linear models developed in the previous section. In general, an excellent agreement between modeled and measured state variables was observed for most runs, confirming that the model of Eqn. 7 and 8 is reasonable. One example from the sea trial is illustrated by Fig. 3 in which measured and modeled roll, yaw, sway, roll rate and yaw rate have been plotted along with the original system input; i.e. $\delta(t)$ as a function of time. With the model in

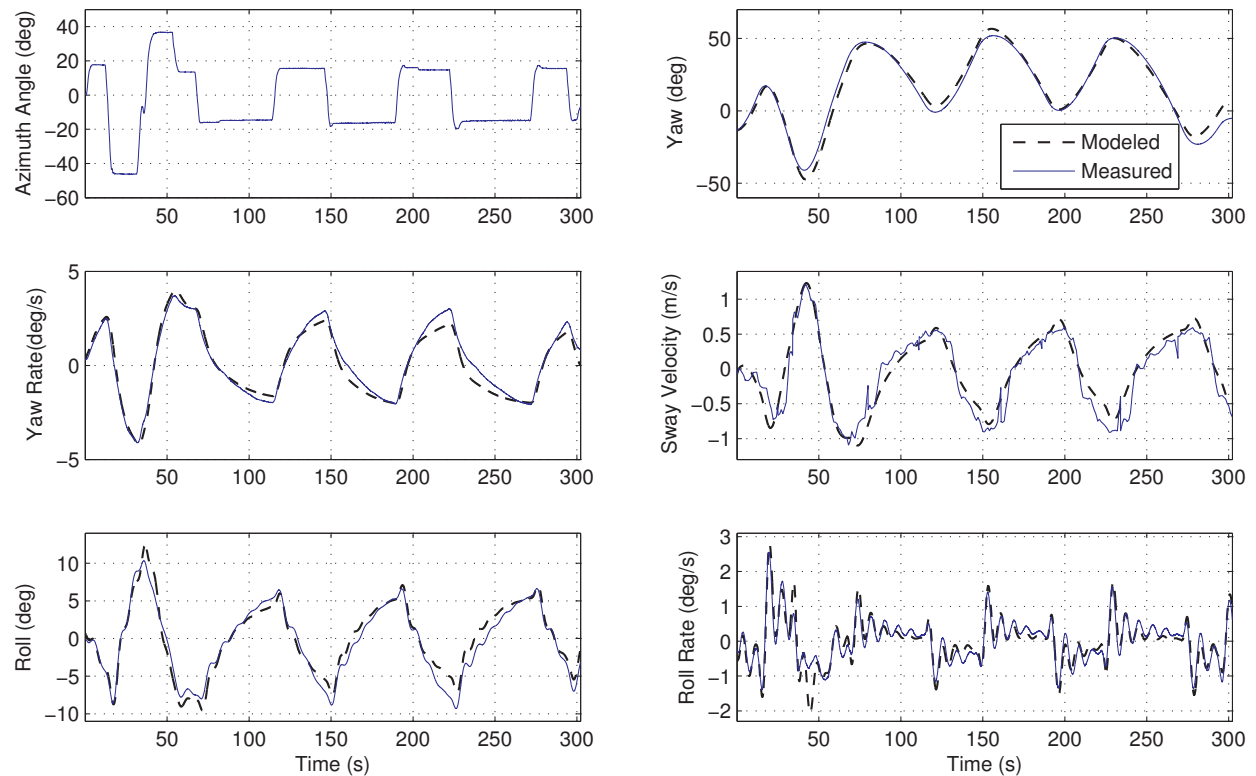


Figure 3: A sea trial run comparing measured to modeled system states

reasonable agreement with the full-scale vessel results, it enables a certain level of confidence to be afforded a control system design based on the model.

4 RESULTS

This section focusses on the results of the system identification of the sea trials: specifically, it will examine the frequency domain behaviour of the system model in roll. Of primary interest are the complex conjugate poles that give rise to the resonant roll mode and the NMP zero. These results are presented in Table 1. The forward speed of the vessel u , and the frequencies of the poles ω_n and the NMP zero ω_z have been normalized by maximum forward speed and maximum frequency encountered, respectively. Normalized speed is denoted as ω_n . These features have been highlighted, since they encapsulate the roll behaviour of the subject vessel over the entire range of service speeds.

4.1 Damping

The damping of the complex conjugate pole pair clearly increases with increasing forward speed; this

Speed u_n	Complex Poles				Zero
	ζ	ω_n	Re	\pm Im	ω_z
0	0.016	0.932	-0.015	0.932	<i>n/a</i>
0.455	0.033	0.952	-0.031	0.951	0.478
0.727	0.084	0.983	-0.083	0.979	0.726
1	0.143	1	-0.143	0.990	0.927

Table 1: Complex conjugate pole pair and non-minimum phase zero. Frequencies and speeds are normalized.

is not a surprising result, as it is likely that hydrodynamic forces at higher speeds contribute to increased roll damping. This relationship is summarized in Fig. 4. The damping increases linearly over the higher range of forward speeds that were tested. At lower speeds, the relation is clearly not linear, but would not be hard to quantify with further testing. A least squares fit of order 2 is superimposed on the points. It should be noted that the damping of these poles is very light and there was some variation between results of the repeated runs for the same speed. The results presented here are an average of what were deemed ‘good quality’ runs; i.e. those in which the SI modeled data matched the actual data closely.

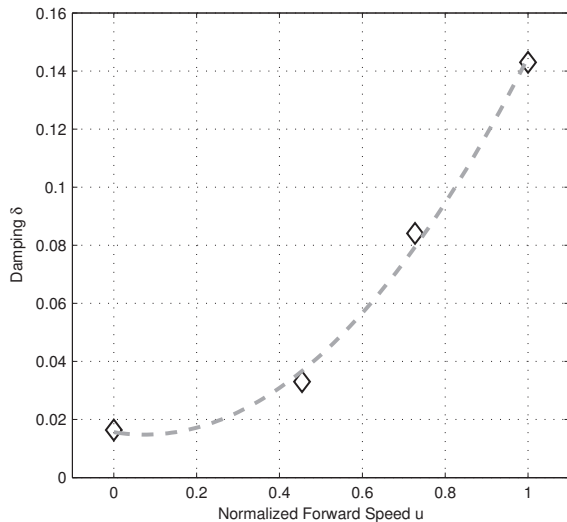


Figure 4: Damping of the complex conjugate pole pair in the roll model as a function of forward speed (normalized). The dashed line is a second-order regression.

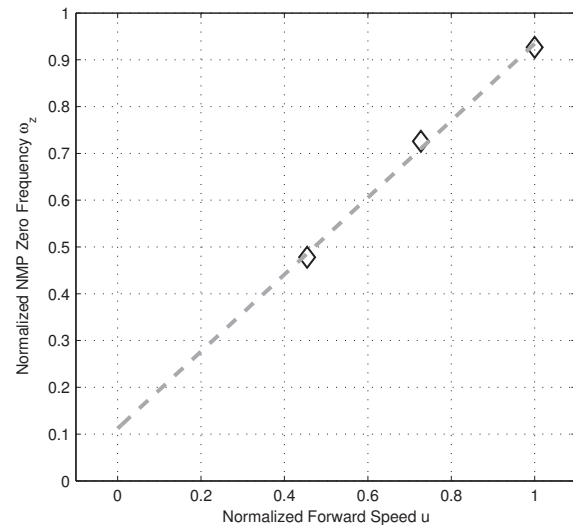


Figure 5: Normalized frequency of the non-minimum phase zero as a function of normalized forward speed. The thicker dashed line is linearly extrapolated to $u_n = 0$.

4.2 Non-Minimum Phase Zero Location

The frequency of the non-minimum phase zero clearly increases with increasing forward speed over the range of speeds tested, see Fig. 5. This is not a surprising result, as the NMP zero can be thought of as a delay element; thus, the faster the vessel moves, the smaller the delay. In Table 1 the *n/a* should be interpreted that the zero is not possible to resolve precisely, as it approaches zero frequency, since for all zero-speed runs analyzed, the zero was in close proximity of the $j\omega$ axis within the confidence limits of the results.

4.3 Control System Discussion

With the open loop model of the system determined, what issues does this raise for a roll stabilizing controller? The discussion will focus only on the implications for roll control, although it should be noted that roll stabilization cannot be considered in isolation of heading (yaw) control. For this discussion, the reader is referred to Fig. 6, the pole-zero plot of the system, with only the complex conjugate pole pair and the NMP zero plotted, for each of the normalized vessel forward speeds, u_n , identified on the plot as the set $\{u_0, u_1, u_2, u_3\}$.

One state-space control design approach is to use the pole-placement technique. The roll natural frequency of the vessel is strongly influenced by its hydrostatics [7].

$$\omega_\phi = \sqrt{\frac{\rho g \nabla GM}{I_{44} - K_p}} \quad (10)$$

It is unlikely that a practical controller gain will be arrived at with an arbitrary pole placement approach (i.e. altering the natural frequency). A better approach is to attempt to increase the damping of the system. The grid in the left hand plane of the pole-zero plot Fig. 6 has lines of equal damping. Thus, the target controller pole positions lie somewhere along the curves for $\omega_n \in (0.932, 1.0)$, adjusting the controller gain to maximize ζ .

The non-minimum phase response (due to the right-half plane zero) manifests itself in the time domain as an initial inverse response to the input. For example, applying helm to initiate a turn to port will cause the vessel to initially roll to the port side, followed eventually by a steady roll (heel) to the starboard side as the turn settles in. This initial inversion gives rise to the NMP zero in the right-hand plane of the system roll transfer function. As the zero moves closer to the $j\omega$ axis at lower speeds, the vessel will exhibit a more pronounced inverse response. Typically from a control systems perspective, NMP dynamics cannot be canceled, and they ultimately lead to a tradeoff between reducing disturbance at certain frequencies, while amplifying them at others. Therefore, the controller must be designed to identify and adapt to varying conditions; e.g. changes in the dominant wave period, and the wave encounter angle.

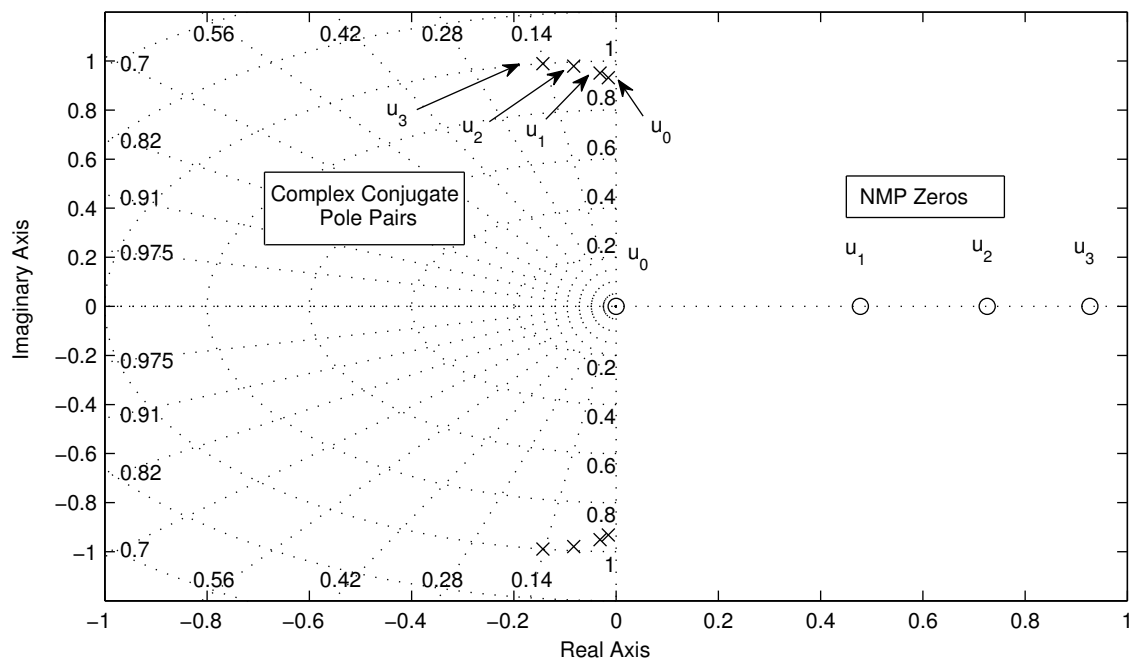


Figure 6: Summary pole-zero map, showing the dependence on forward speed. The grid in the left hand plane indicates lines of equal damping.

A serious limitation of this vessel as a candidate for ZRS will be at the highest speed u_3 ; the natural frequency of roll coincides with the frequency of the NMP zero, making roll reduction at that speed particularly problematic. At speeds below this, there is sufficient separation between ω_n and ω_z that the NMP effect will be less dominant by carefully limiting the bandwidth of the controller to frequencies above ω_z . As the vessel speed gets lower, the separation increases, making ZRS likely to be more effective at lower speeds. At zero speed u_0 the side thruster actuator mode can be utilized and the NMP zero disappears, making the control problem considerably easier to handle.

5 CONCLUSIONS

This paper presents a technique for deriving linear vessel manoeuvring models for control system design based on system identification of sea trials data. By basing a controller design on an identified model, the designer will have more assurance that the resulting controller will work with the real vessel. A technique for improving the actuation of a ZRS control system is presented; by manipulating both the azimuth angle and the shaft speed, it is possible to get around one of the serious limitations (i.e. underactuation) of rudder-

based control systems. Finally, the NMP dynamics of the system are less problematic at low speeds and disappear at zero speed. This is a range of operation in which traditional RRS systems cannot function due to loss of lift on the rudder. These observations form the preliminary design phase of an integrated yaw and roll controller using Z-drives.

Future work will use the information gleaned in this modeling process to do the detailed design of a controller for the vessel using a variety of control design approaches. The performance of the controllers will be evaluated using simulation techniques against either a nonlinear SI model derived from the sea trials data, or a nonlinear model derived from first principles.

ACKNOWLEDGEMENTS

The authors would like to acknowledge the support of this research by Mr. Mike Dervin of the Canadian Department of Defence, Directorate of Maritime Ship Support (DMSS).

REFERENCES

- [1] M. Blanke and M. Knudsen. A sensitivity approach to identification of ship dynamics from

- sea trial data. In *Proceedings of the IFAC Conference on Control Applications in Marine Systems, CAMS'98*, pages 261–269, Fukuoka, Japan, October 1998. IFAC.
- [2] A. Christensen and M. Blanke. A linearized state-space model in steering and roll of a high-speed container ship. Technical Report 86-D-574, Servolaboratoriet, Technical University of Denmark, 1986.
- [3] W. E. Cowley and T. H. Lambert. The use of rudder as a roll stabilizer. In *Proceedings of the 3rd International Ship Control Systems Symposium*, Bath, UK, 1972.
- [4] W. E. Cowley and T. H. Lambert. Sea trials on a roll stabiliser using the ship's rudder. In *Proceedings of the 4th Ship Control System Symposium - SCSS*, The Netherlands, 1975.
- [5] T. I. Fossen. *Marine control Systems - Guidance, Navigation and Control of Ships, Rigs and Underwater Vehicles*, chapter 9. Marine Cybernetics, 2002.
- [6] L. Ljung. *System Identification Theory for the user*. Information and System Sciences. Prentice-Hall, 1987.
- [7] T. Perez. *Ship Motion Control: Course Keeping and Roll Stabilisation Using Rudder and Fins*. Advances in Industrial Control. Springer, 1 edition, August 2005.
- [8] R. Taggart. Anomolous behaviour of merchant ship steering systems. *Marine Technology*, pages 205–215, April 1970.
- [9] E. Thornhill, D. Bass, and J. Millan. Numerical prediction of z-drive roll reduction capability. In *Proceedings of the 6th International Ship Stability Workshop*, New York, October 2002. Webb Institute.
- [10] J. van Amerongen and J. C. van Cappelle. Mathematical modeling for rudder roll stabilization. In *Proceedings of the 6th International Ship Control Systems Symposium*, Ottawa, Canada, 1981.